forests

MDPI

Article

Seven Millennia of *Cedrus atlantica* Forest Dynamics in the Western Rif Mountains (Morocco)

Francisca Alba-Sánchez [1], Daniel Abel-Schaad [1,*], José Antonio López-Sáez [2], Daniel Romera-Romera [3], Sebastián Pérez-Díaz [4] and Antonio González-Hernández [1]

[1] Department of Botany, University of Granada, 18012 Granada, Spain; falba@ugr.es (F.A.-S.); aglezhdez@gmail.com (A.G.-H.)
[2] Research Group Environmental Archaeology, Instituto de Historia (CSIC), 28037 Madrid, Spain; joseantonio.lopez@cchs.csic.es
[3] Department of Botany, Ecology and Plant Physiology, University of Córdoba, 14071 Córdoba, Spain; b62rorod@uco.es
[4] Department of Geography, Urban Planning and Land Management, University of Cantabria, 39005 Santander, Spain; sebastian.perezdiaz@unican.es
* Correspondence: dabels@ugr.es

Abstract

Atlas cedar (*Cedrus atlantica* (Endl.) Manetti ex Carrière) is an endemic and relict conifer species from northwestern Africa, relatively drought-tolerant but also highly sensitive to recurrent summer heat stress. Cedar forests have undergone a dramatic range contraction in recent decades. The development of effective conservation strategies requires long-term perspectives to understand how forests have responded to past disturbances. We present a multi-proxy, high-resolution analysis of a 122 cm-deep fossil record (Merj Lkhil; LKH) located at 1213 m a.s.l. in Jbel Bou Hachem (Moroccan Rif), providing insights into the fragmentation of cedar stands. *Cedrus* likely formed extensive lowland populations during the final stages of the Late Glacial and began migrating upslope during the Greenlandian. It reached its maximum extent in the Rif around 7000 cal yr BP. Thereafter, increasing aridity, enhanced seasonality, and growing anthropogenic pressure triggered its long-term decline. This trajectory involved a vertical reorganization of montane ecosystems, with *Cedrus* progressively retreating within mid- and low-elevation forests, while deciduous oaks maintained a long-term co-dominance and *Q. ilex* L. gradually expanded, especially at lower elevations. Today, *Cedrus* is confined to isolated high-elevation stands in Jbel Bou Hachem. These relic populations should be prioritized for conservation under ongoing climate and land-use change.

Keywords: Atlas cedar; climate threat; Holocene; human impact; Mediterranean forests; resilience

Academic Editor: Ernesto I. Badano

Received: 7 August 2025
Revised: 28 August 2025
Accepted: 8 September 2025
Published: date

Citation: Alba-Sánchez, F.; Abel-Schaad, D.; López-Sáez, J.A.; Romera-Romera, D.; Pérez-Díaz, S.; González-Hernández, A. Seven Millennia of *Cedrus atlantica* Forest Dynamics in the Western Rif Mountains (Morocco). *Forests* **2025**, *16*, x. https://doi.org/10.3390/xxxxx

1. Introduction

Mountains host high levels of diversity and endemism due to the heterogeneity of their abiotic conditions [1,2], which underscores their essential role as cradles, bridges, and reservoirs for many species that are often isolated by surrounding lowlands [3]. This pattern is especially evident in the Mediterranean Basin, one of the world's major biodiversity hotspots, where plant richness is especially concentrated in mountain regions [4],

with one main centre located in the west, including the Baetic ranges (Iberian Peninsula) and the Atlas and the Rif mountains in Morocco [5].

Cedrus atlantica (*Atlas cedar*) is among the most emblematic and ecologically significant conifer species in the Mediterranean region. It is considered intermediate-temperate in its climatic affinities [6], moderately drought-tolerant, highly sensitive to recurrent summer heat stress [7], and physiologically vulnerable under projected warming scenarios. Although this conifer is relatively resistant to moderate drought, it becomes increasingly susceptible to prolonged dry periods and heat stress due to its shallow roots, reduced stomatal control, and limited thermal tolerance [8,9]. Cedar forests develop under a Mediterranean-type (Csa) climate [10] and are typically included in the Mediterranean Woodland and Scrub biome within the broader category of Temperate Forests [11,12]. However, their classification remains ambiguous, as they share features with warm, cool, and even boreal forest types [13], highlighting the ecological singularity of this species.

Today, Atlas cedar populations are restricted to mountain areas in Morocco and Algeria, with approximately 80% of their range located in the Middle Atlas [14]. In the Rif Mountains, forests of *Cedrus atlantica* cover about 12,000 ha, scattered across six main populations situated between 1400 and 2300 m a.s.l., spanning roughly 120 km from Jbel Tidighine in the east to Jbel Bouhachem in the west [15]. These populations are currently undergoing a process of decline, which is expected to intensify in the coming decades due to increasing aridity and temperatures as well as human disturbance, leading to habitat degradation, biodiversity loss, and a shift in forest composition [16,17]. *Cedrus atlantica* is currently listed as Endangered on the IUCN Red List [18].

Palaeoecological evidence from the Rif Mountains and surrounding areas indicates that *Cedrus atlantica* spread extensively between ca. 11,000 and 6000 cal yr BP [19–21], maintaining a substantially broader distribution until the mid-Holocene, especially at lower elevations, compared to its current range [15]. This distributional shift was facilitated by favourable climatic conditions, notably higher water availability and cooler winters, which allowed cedar populations to occupy a wider altitudinal and geographic range across the region.

From around 6000 cal yr BP onwards, a shift towards drier and warmer conditions triggered a gradual contraction of its distribution and an upward migration. Cedar pollen steadily declined in all records, and local extinctions occurred at lower elevations [15,22]. Palaeoecological records show a sequential shift in forest composition particularly at mid-elevations, initially, more drought-tolerant broadleaved species such as *Quercus* L. became dominant [23]. With ongoing aridification and intensified land use, these forests were gradually replaced or interspersed with xerophytic taxa, including *Cistus* L. and *Juniperus* L., especially in degraded areas [22]. Over time, this transformation led to more open and structurally simplified landscapes [24], a pattern also observed today in degraded cedar stands in the Middle Atlas under similar pressures [9]. While these shifts were historically gradual, future climate projections for the Atlas Mountains suggest that, under scenarios of declining precipitation by 20%–30% and 2 °C raise on temperature, forested zones above 1600 m could shift toward treeless, low-diversity steppes dominated by scattered xerophytic taxa [16].

The responses of cedar forests to past disturbances have varied across the different massifs of the Rif mountain range. While in the easternmost areas (e.g., Jbel Tidighine) cedar forests have persisted occupying large areas [25], in the westernmost area of the Rif mountains, such as Jbel Khesana, they became completely extinct after dominating the landscape until recent millennia [15,22,23,26]. Today, only a few isolated stands survive at higher elevations in the western Rif, one of which is the population under study in Jbel Bou Hachem.

Long-term palaeoecological records offer a critical framework for interpreting these vegetation dynamics, enabling researchers to identify thresholds of ecological resilience or episodes of structural reorganization. These records are particularly relevant to conservation, offering temporal depth to assess ecosystem vulnerability and guide adaptive strategies in the face of ongoing climate change [27]. In the western Rif Mountains, this approach is especially useful for identifying persistent forest populations and potential microrefugia, such as those found at Jbel Kelti, Tiziren and Talassemtane [28]. These relict stands may hold long-term ecological and genetic value, especially under scenarios of increasing climate stress [28].

We present here a new high-resolution multiproxy palaeoecological record from Merj Lkhil, a peatland located in Jbel Bouhachem, within the Rif Mountains of northern Morocco. The 7000-year core was taken from a site located at higher elevation than other sequences previously studied in the Jbel Bou Hachem (Maison Forestière 1 and 3: [29,30] and M'Had: [15]). Our record provides an opportunity to reconstruct the Holocene dynamics of *Cedrus atlantica* at its northwestern ecological margin and to assess how forest composition shifted in response to rising temperatures, increasing aridity, and anthropogenic disturbance. In addition, we conducted a review of previous palaeoecological studies in the Rif Mountains to contextualize our findings and to address the following objectives: (1) to document the structural and compositional transformation of cedar forests in the western Rif Mountains; (2) to identify the timing and drivers of replacement by broadleaved and xerophytic species; (3) to assess the implications of these changes for long-term ecosystem resilience and conservation planning.

2. Materials and Methods

2.1. Study Area

The mire of Merj Lkhil (LKH: 35°15′13″ N, 5°25′56″ W) is located at 1213 m a.s.l. (Figure 1) in the northern slope of Jbel Bouhachem, whose maximum elevation reaches 1681 m a.s.l., taking part of the Oligo-Miocene sandstone formation of the Rif mountains, which originates siliceous soils [31]. The climate is Mediterranean shaped nuanced by a noticeable Atlantic influence. Winters are wet and cool and summers warm and dry, with a mean annual temperature ~17 °C and mean annual rainfall higher than 2000 mm [31]. There is a marked decreasing rainfall gradient from West to East in the Rif mountains [32].

This wetland has been categorized as a "Sphagnum pond" [30], flooded during winter and spring, covered by *Sphagnum auriculatum* Schimp. Other species found are *Baldellia ranunculoides* (L.) Parl., *Danthonia decumbens* (L.) DC., *Eleocharis* R. Br. spp., *Exaculum pusillum* (Lam.) Caruel., *Gratiola mauretanica* (Emb. & Maire) I.Soriano & T.Romero., *Juncus bulbosus* L. and *Potentilla erecta* (L.) Raeusch.

Altitude plays a key role in shaping tree species composition and abundance in northern Morocco, primarily through its influence on microclimatic variation and species-specific tolerance to cold stress [31]. In this sense, three bioclimatic belts have been described in the western Rif mountains (Figure 2), each represented by a specific vegetation [14,32,33]. Cork oak (*Quercus suber* L.) forests dominate the Thermomediterranean belt (~100–800 m a.s.l.), with a significant presence of holm oaks (*Q. ilex*) and olive trees (*Olea europaea* L.). The Mesomediterranean belt (~800–1300 m a.s.l.) includes cork (*Q. suber*), zeen (*Q. canariensis* Willd.) and pyrenean (*Q. pyrenaica* Willd.) oak forests distributed according to moisture and soil requirements, with a well-developed understorey mainly composed by taxa belonging to Fabaceae, Ericaceae and Cistaceae. In the Supramediterranean belt (~1300–1700 m a.s.l.) pyrenean oaks (*Q. pyrenaica*) become more dominant with increasing altitude, accompanied by ferns like *Pteridium* Gled. ex Scop.and taxa mainly belonging to Cistaceae. On the top of this belt (~1515 m.a.s.l), a stand of cedar

(*Cedrus atlantica*) shows the last remains of these forests in Jbel Bouhachem (Figure 3), characterized by the significant presence of holly (*Ilex aquifolium* L.). The recent impact of human activities has originated a high biodiversity loss, triggering a wide landscape opening and the depletion of tree cover [34]. In 2006 UNESCO declared the Andalusia-Morocco Intercontinental Biosphere Reserve, of which the Bou Hachem Regional Natural Park forms part.

Figure 1. Location of Merj Lkhil (LKH), showing the main ridges some previous palaeoecological studies cited in the text located in the Jbel Bou Hachem: M'Had (MHA) [15], Maisson Forestiere 1 (MF1), Maisson Forestiere 3 (MF3) [29,30]; and surroundings areas Bab El Karn (BEK) [23]; Bab el Karn II (BEK2) [22]; Archaeological Sites (Blue triangles): Kaf Taht-el-Ghar (KTG) [20]; Ifri Oudadane (OUD) [21]; Ifri El Baroud (BAR) [35]; Ifri n'Etsedda (NET) [19]; Taforalt (TAF) [36].

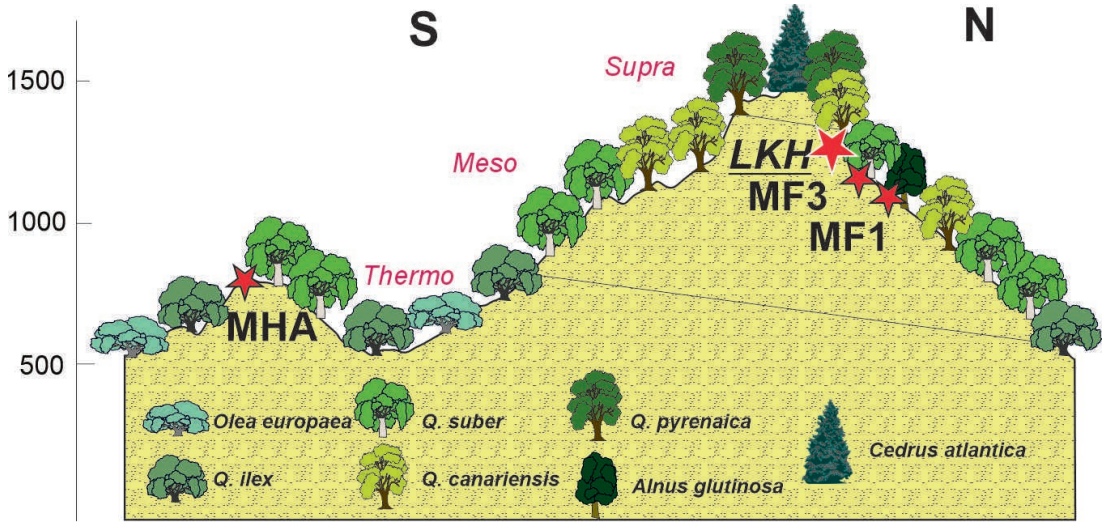

Figure 2. Schematic diagram showing the vegetation communities in the Jbel Bou Hachem and the location of the records of M'Had (MHA) [15], Maison Forestiere 1 (MF1), Maison Forestiere 3 (MF3) [29,30] and Merj Lkhil (LKH; this study).

Figure 3. Last extant population in Jbel Bou Hachem, on a summit at 1515 m a.s.l.

2.2. Coring and Chronology

Samples were obtained from a 122 cm core extracted in 2016 with a Russian corer. They were then sub-sampled at 1 cm intervals for subsequent analyses.

Six radiocarbon datings were performed on bulk peat samples at the Poznań Radiocarbon Laboratory (Table 1). The IntCal20 ^{14}C curve [37] was used to calibrate ages BP. Confidence intervals at 95% (2σ) were calculated for the calibrations and the age–depth model (Figure 4), where a smooth-spline solution was applied with Clam 2.2 software [38].

Table 1. Results of Radiocarbon (^{14}C) dating of LKH samples, showing calibrated age ranges (2σ).

Depth (cm)	Lab Code	^{14}C Age	Age cal yr BP		Probability	Median
			Min	Max		
25	Poz-136570	580 ± 30 BP	505	554	91.6	528.2
			611	620	3.2	
40	Poz-136571	1385 ± 30 BP	1276	1343	95	1309.5
55	Poz-136497	2410 ± 30 BP	2351	2496	81.2	2458.7
			2596	2612	2.9	
			2637	2684	10.9	
75	Poz-136498	4175 ± 30 BP	4588	4594	1	4716
			4614	4766	73.1	
			4783	4833	20.8	
95	Poz-136499	5350 ± 40 BP	6001	6216	85.2	6124.8
			6239	6271	9.7	
121	Poz-82284	6150 ± 50 BP	6904	7169	95	7036.5

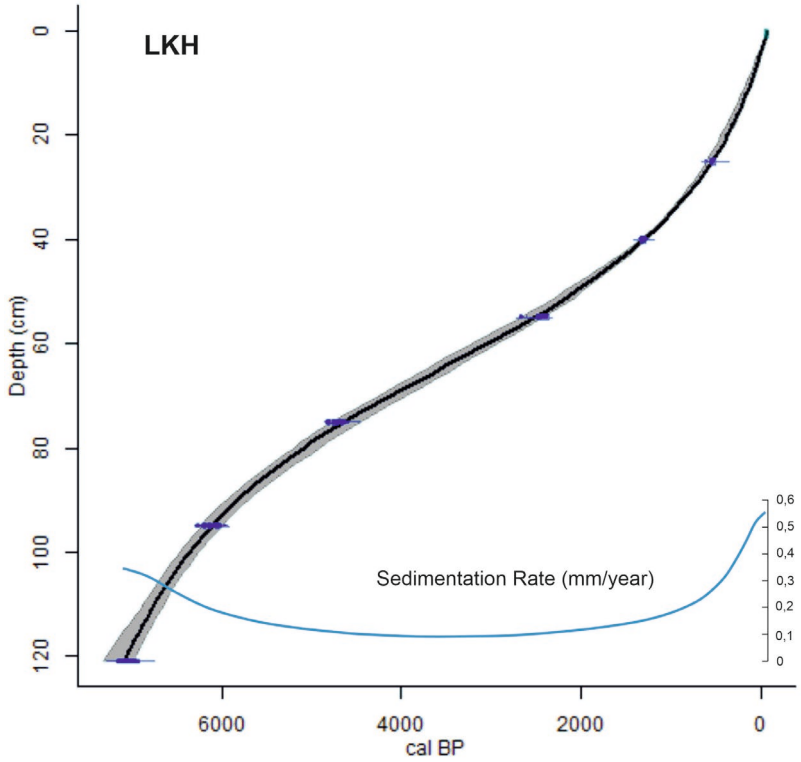

Figure 4. Age–depth model for LKH mire.

2.3. Pollen Palynomorphs, NPPs and Charcoal Analyses

The traditional chemical treatment [39] was employed on the samples, using Thoulet solution for separating to separate pollen and Non-pollen Palynomorphs (NPPs) from the rest of the sediment [40]. *Lycopodium* tablets were also added to estimate pollen concentration [41]. Data processing and graphic representation were performed with TILIA 2.6.1 software, which includes a cluster analysis (CONISS) to determine Local pollen assemblage zones. Pollen grains were identified according to several keys [39,42] and pollen atlases [43]. Local pollen types, such as hydro-hygrophilous taxa, ferns and NPPs were excluded from the total pollen sum (>500 pollen grains). The identification and nomenclature of NPPs is based on [44] and references therein. Charcoal accumulation rate (CHAR) was also estimated from the counts of microcharcoal in the pollen slides [45], dividing its concentration by the sedimentation rate of each sample from the age-depth model [46].

We used Principal Component Analysis (PCA) to identify the main gradients of long-term vegetation dynamics, including taxa with a minimum abundance of 5%. Pollen percentages were square-root transformed and the ordination was performed with PAST [47].

The first included diagram (Figure 5) shows pollen and NPPs grouped according to their ecological affinities (Table 2), with diverse charts on the right, respectively, displaying CHAR, the relation between Arboreal (AP) and Non-Arboreal Pollen (NAP), the Sedimentation and Pollen Accumulation Rates (PAR) throughout the four subzones. In addition, we have included the results of the PCA principal components and of the paleoclimatic reconstruction, as well as some graphs extracted from some previous climate-related works in the area (Figure 6) and, finally, the Anthropogenic Pollen Index developed by [48]. A detailed pollen diagram has also been included as supplementary material (Figure S1).

We inferred local presence of the main arboreal taxa using percentage thresholds (e.g., *Cedrus atlantica* > 7%, deciduous *Quercus* > 15%–20%, *Q. ilex* > 20%), based on empirical ranges observed in mediterranean montane environments [49].

Table 2. Groups of pollen and non-pollen palynomorphs according to their ecological affinities.

Group	Pollen Types and Non-Pollen Palynomorphs
Riparian woods	*Alnus*, *Prunus*, *Salix*
Thermophilous shrubland	*Cistus*, *Cytisus*, *Erica arborea*, *Helianthemum*, *Ilex*, *Phillyrea*, *Viburnum*
Anthropogenic Perennial Pastures (APP)	*Apiaceae*, *Artemisia*, *Caryophyllaceae*, *Fabaceae*, *Liliaceae*, *Lotus*, *Rosaceae*
Anthropogenic Nitrophilous Communities (ANC)	*Anthemis*, *Asphodelus albus*, *Aster*, *Cardueae*, *Cichorioideae*
Anthropozoogenic Nitrophilous Communities (AZNC)	*Amaranthaceae*, *Plantago* spp., *Rumex* spp.
Aquatic taxa (AT)	*Myriophyllum*, *Ranunculaceae*
Open water (OW)	*Mougeotia*
Coprophilous fungi (CFs)	HdV 7A, HdV 55A, HdV 112, HdV 113, HdV 172, HdV 368
Dry conditions	HdV 16
Erosive phases	HdV 207 *(Glomus)*, *Pseudoschizaea circula*

2.4. Paleoclimate Reconstruction

The paleoclimate (i.e., temperature and precipitation) reconstructions (Figure 6) were obtained from the dsclim dataset [50]. This dataset is the result of a perfect prognosis downscaling (i.e., based on the construction of a transfer function between high-resolution data and low-resolution data for each high-resolution pixel.) using UERRA reanalysis (https://www.uerra.eu/, accessed on 16 September 2024) and TraCE 21 ka (https://www.earthsystemgrid.org/project/trace.html) (accessed on 16 September 2024) datasets focused on the western Mediterranean Area. For further methodological details, please see documentation of the dsclim R-package (https://www.dnietolugilde.com/dsclim, accessed on 16 September 2024). The dataset provides monthly data from 22 ka BP to 1990 at a spatial resolution of 11 × 11 km. Furthermore, the mean monthly temperature and precipitation values from the overlapping pixel with the site (LKH) was extracted for the same period (from 7118 to 0 years cal yr BP). To avoid seasonal and annual fluctuations, both data series were smoothed by calculating the average with a 100-year moving window.

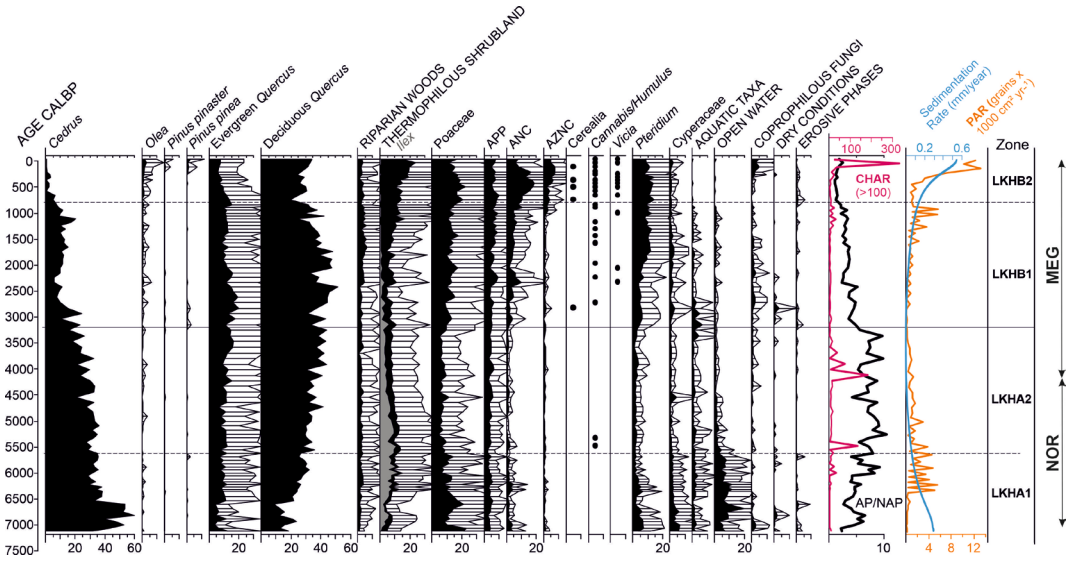

Figure 5. Summary diagram including selected pollen types, Non-Pollen Palynomorphs, Charcoal Accumulation Rate (CHAR), Arboreal vs. Non-arboreal pollen (AP/NAP), and Sedimentation and

Pollen Accumulation (PAR) rates, Principal Components (PC1/PC2), Paleoclimate reconstruction (TEMP/PREC), climate proxies from previous works [51–55] and Anthropogenic Pollen Index (API) [48].

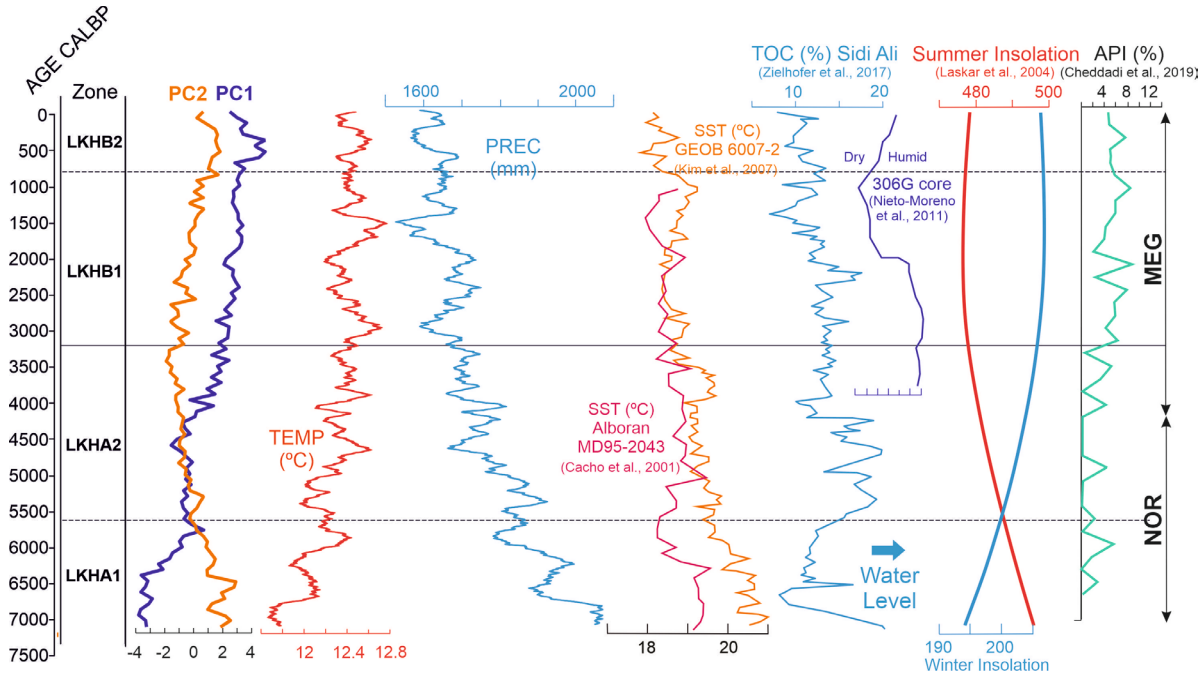

Figure 6. Summary diagram including Principal Components (PC1/PC2), Paleoclimate reconstruction (TEMP/PREC), climate proxies from previous works [51–55] and Anthropogenic Pollen Index (API) [48].

3. Results

Two main pollen zones were identified (Figure 5) which were divided into four subzones, with their own characteristics (Table 3), using a constrained cluster analysis included in TILIA 2.6.1.

Table 3. Description of pollen zones.

SUBZONE Depth (cm)/Age cal BP	Trees/Thermophilous Shrubland (ThSh)	Herbs	Ferns/Hygrophytes/Aquatic Taxa/Open Water Algae (OW)	NPPs/CHAR/Pollen Concentration (CC)
LKHA1 122–88 cm ~7118–5625 cal BP	AP/NAP ~5 Maxima of *Cedrus* (~60%) ~6800 cal BP and medium levels thereafter (~33%) Increasing levels of both evergreen (~9%) and deciduous (~29%) *Quercus*, as well as ThSh (4%–10%) Low levels of Riparian woods (~2%) Sporadic occurrences of *Pinus* and *Olea*	Decreasing percentages of Poaceae (21%–14%) Low levels of APP (~4%), ANC (~2%) and AZNC (<1%)	Decreasing levels of *Pteridium* and Cyperaceae Maxima of OW	Sporadic occurrences of Coprophilous fungi Low levels of CHAR Initial minima of Pollen CC
LKHA2 88–62 cm ~5625–3199 cal BP	AP/NAP ~7.5 Steady decrease in *Cedrus* (31%–21%) against evergreen (11%–14%) and deciduous (36%–41%) *Quercus* Low levels of Riparian woods (~2.5%) Sporadic occurrences of *Olea* Slight decrease in ThSh (~12%–8%)	Minima of Poaceae (~7%), ANC (~1%) and AZNC (<1%) APP remain (~4%)	Low levels of *Pteridium* and Cyperaceae Low levels of OW and Aquatic Taxa with a final peak	Sporadic occurrences of Coprophilous fungi Significant peaks of CHAR ~5500 and 4150 cal BP Decreasing pollen CC
LKHB1 62–32 cm ~3199–793 cal BP	AP/NAP ~3.5 Steady decline of *Cedrus* (~18%–9%) Initial maxima of evergreen (20%) and deciduous (51%) *Quercus* and subsequent slight decrease	Increasing percentages of Poaceae (~11%–13%), APP (~5%–7%), ANC (~3%–7%) and AZNC (>2%)	Increasing levels of *Pteridium* and decline of Cyperaceae Initial significant levels of Aquatic Taxa and subsequent decrease Low levels of OW	Continuous levels of Coprophilous fungi Initial peaks of Dry phases Low levels of CHAR with slight final peaks Increasing Pollen CC

	Increasing levels of *Olea*, Riparian woods (~3.5%) and ThSh (~8%–12%)	First occurrences of Cerealia, *Cannabis* and *Vicia*		
LKHB2 32–2 cm ~793 cal BP-present	AP/NAP ~2.6 Demise of *Cedrus* Decrease in evergreen (~12%–7%) and increase in deciduous (~25%–31%) *Quercus* after an initial decline Increase in *Olea* (~2%) and *Pinus* (>1%) Maxima of ThSh (~19%)	Maxima of Poaceae (~22%), APP (~10%), ANC (~19%) and AZNC (~8%) More continuous occurrences of Cerealia, *Cannabis* and *Vicia*	Maxima of *Pteridium* and low levels of Cyperaceae Virtual demise of both Aquatic Taxa and OW	Maxima of Coprophilous fungi and increase in Erosive phases Final maximum of CHAR Increasing Pollen CC

CHAR: charcoal accumulation rate; AP: arboreal pollen; NAP: Non-Arboreal pollen.

These pollen subzones are also shown in the PCA biplot (Figure 7), which defines two principal components. PC1 accounts for 62.3% of the total variance in the data set, and shows moderate positive loadings of ANC, *Pteridium*, AZNC and Poaceae, as well as strong negative loadings of *Cedrus*, OW and AQ. This axis can be interpreted as an aridity gradient, as it corresponds closely with the declining precipitation curve shown in the palaeoclimate reconstruction (Figure 6). PC2 explains 15.4 % of the variance, with high positive loadings of ANC, OW, Poaceae, ANC and *Pteridium* and strong negative loadings of deciduous and evergreen *Quercus*, likely reflecting a gradient of landscape openness.

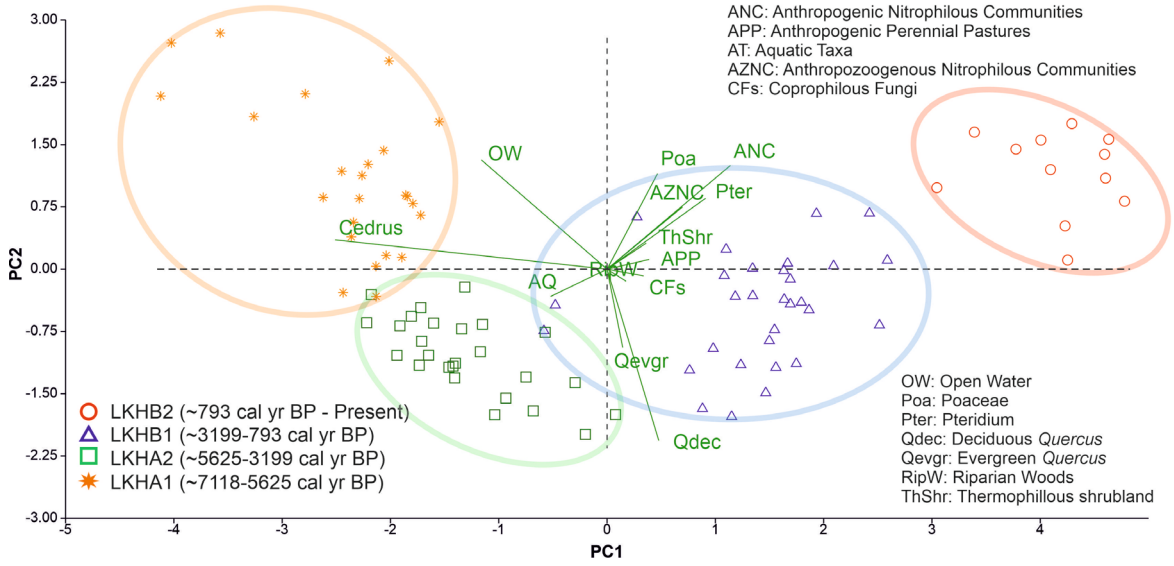

Figure 7. PCA biplot with samples (figures) and pollen and non-pollen groups from LKH mire. Pollen subzones obtained with TILIA are also shown and marked.

4. Discussion

4.1. The Maximum Expansion of Cedar Forests at the Mid-Elevation Mountain Site—Subzone LKHA1 (122–88 cm; ~7118–5625 cal yr BP)

This basal subzone starts during the first stages of the Northgrippian (NOR) in the western Mediterranean [56]. The previous Greenlandian was a phase of wetter conditions [57] enough to promote the gradual expansion of cedar forests in the Rif mountains and surrounding areas, particularly at lower elevations [15]. The NOR, by contrast, shows a progressive shift to drier and cooler conditions, not only in this area, but also in the Mediterranean region, nuanced by seasonal changes affecting both rainfall and insolation [22,51,53]. This trend is also reflected in our site-specific paleoclimatic reconstruction (Figure 6), which shows a gradual decline in precipitation (PREC) and slightly increasing temperature (TEMP) during this subzone, consistent with regional patterns in terms of

precipitation, but not so much in relation to temperatures, which shows the more local nature of the climate in mountainous areas.

During this phase, the area of LKH was extensively flooded, as indicated by the high levels shown by Open Water (OW) indicators (Table 3; Figure 5). This hydrological setting is consistent with the climate conditions described for the first stages of NOR in the area [15], helping the widest development of cedar forests at this altitude, likely forming relatively dense and well-structured forests at mid-elevation, which also characterizes this phase, along with a well-developed shrub layer in which *Ilex* appears as a key component. Grasslands are mainly composed of Poaceae with a low but significant contribution of perennial pastures and nitrophilous communities (Figure 5). Tree cover, as shown by AP/NAP ratio was relatively high in these first stages, likely due to these initial favourable climate conditions, especially for Atlas cedar.

A noteworthy change is observed around 6600 cal yr BP, marked by a pronounced decline in *Cedrus* pollen, indicating a reduction in arboreal cover. This is followed by the gradual expansion of oak forests, predominantly deciduous species. The increasing aridity characteristic of the NOR may underlie this vegetation shift, evidenced by a rise in Aquatic Taxa (AT) relative to Open Water (OW) algae (Figure 5), suggesting a lowering of the water table, also reported in other records [53], likely due to the sharp drop in rainfall, as indicated by the site-specific paleoclimate reconstruction (Figure 6). In response to these conditions, cedar populations likely retreated, while mainly deciduous oaks—and, more rarely, evergreen oaks restricted to drier exposures—progressively expanded, probably occupying the lower elevational range previously held by cedar forests [16]. This replacement can be explained by the greater physiological tolerance of *Quercus* species to prolonged summer drought than *Cedrus* [8,9]. Ref. [16] also report a sedimentological change at ~6800 cal yr BP, attributed to climatic forcing rather than human influences. The widespread expansion of oaks and thermophilous shrubland points to a subsequent increase in climatic seasonality, which may have facilitated fire activity during the final stages of this subzone, as indicated by small peaks in CHAR values (Figure 5).

Samples from subzone LKHA1 are clustered on the upper-left quadrant of the PCA biplot (Figure 7), closely aligned with *Cedrus* and aquatic indicators, suggesting humid conditions and dense local forests. The upward distribution along PC2 may reflect increasing arboreal cover, while their position away from disturbance and *Quercus* vectors supports a relatively undisturbed, *Cedrus*-dominated ecosystem.

Meanwhile, the earliest evidence of human presence in the northwestern Moroccan lowlands dates to around 7000 cal yr BP [20,58,59] whereas traces of anthropogenic activity in the Rif Mountains appear considerably later, as indicated by the Anthropogenic Pollen Index (API) described by [48]. The presence of low but significant levels of Coprophilous Fungi (CFs) in this subzone (Figure 5) should be then attributed to wild herbivores, without ruling out any kind of livestock in the area.

4.2. Cedar-Oak Transition and Early Human Disturbance Under Increasing Climatic Stress—Subzone LKHA2 (88–62 cm; ~5625–3200 ca yrl BP)

This interval (5625–3200 cal yr BP) falls within a broader regional climatic context characterized by progressive aridification, declining sea surface temperatures, increased climatic seasonality (drier summers and colder winters), and a persistently positive North Atlantic Oscillation (NAO) phase [51–53,56]. The start of this subzone is marked by the transition from a permanent to a temporary pond in the study area, as shown by the sharp drop in OW algae and the concurrent slight increase in Aquatic Taxa (AT) and Cyperaceae (Figure 5), likely related to the NOR increasing aridity [53] as also shown by the site-specific paleoclimate reconstruction (Figure 6). In addition, a turning point is recorded in this transitional phase from NOR to the Meghalayan (MEG), when the seasonal curves of

insolation crossed (Figure 6), indicating a shift in seasonal climatic dynamics, which may have favoured forest expansion over grasslands at this elevation.

More specifically, these climatic conditions appear to have favoured, particularly since ~4500 cal yr BP, the development of oak forests, namely deciduous ones, at the expense of cedar populations, which would have migrated upwards in search of more optimal conditions, possibly driven by increasingly drier summers and seasonality [51,52,55,56]. This shift is also reflected in the composition of the thermophilous shrubland, where *Ilex*, often associated with cedar forests, loses prominence in favour of more xerophytic taxa such as *Cytisus*, *Cistus*, or *Erica* (Figure 5), which are typically linked to oak-dominated environments. Forests cover reaches a maximum during this phase, as shown by the peak AP/NAP (Table 3, Figure 5), with a co-dominance of cedar and oak taxa. Throughout the subzone, these taxa appear to gradually segregate into distinct vegetation belts, suggesting a slow structural differentiation similar to that observed in other parts of the Rif [22,26]. Following this trend, evergreen *Quercus* shows a slight increase in representation towards the end of the interval, supporting the interpretation of a gradual altitudinal differentiation in forest composition within the area.

This phase of relative ecological stability was only disrupted by the occurrence of fire events, as indicated by two distinct peaks in CHAR values (Figure 5). The first peak appears more likely associated with heightened climatic seasonality, given the near absence of other anthropogenic indicators—despite the first appearance of *Cannabis/Humulus* pollen, which is more plausibly attributed to *Humulus lupulus*, a typical component of alder woodlands in the region. Signs of human impact become more evident towards the onset of MEG in the Rif mountains [48]. This is also reflected in LKH by the co-concurrence of a second peak of CHAR, slight increases in CFs, nitrophilous communities (both ANC and AZNC) and *Pteridium*, linked to forest clearings (Figure 5). Anyway, this human influence is still weak at this stage, and climate continues to be the dominant driver of vegetation dynamics, as suggested by the consistently low values of the Anthropogenic Pollen Index (API).

The PCA biplot (Figure 7) supports a local thermophilization trend, evidenced by the increased presence of warm-adapted taxa in the assemblage [60]. This pattern is consistent with the site-specific reconstructed temperature rise observed in this subzone (Figure 6) and suggests a compositional shift favouring thermophilous species. During this phase, cedar forests are progressively replaced by denser oak woodlands, still developing under relatively humid conditions. The rightward shift in sample scores on PC1 reflects increasing aridity, in agreement with the progressive decline in precipitation documented in the paleoclimate reconstruction (Figure 6).

4.3. Increasing Human Activity Is Becoming the Main Driver of Tree-Cover Loss—Subzone LKHB1 (62–32 cm; ~3200–800 cal yr BP)

The transition to this subzone is marked by the lowest Pollen Accumulation Rate (PAR), which has been related to reductions in forest biomass [61,62]. The simultaneous sharp decline in the AP/NAP ratio (Figure 5) suggests environmental stress limiting forest development. The progressive strengthening of aridity could be responsible of such changes [53], with precipitation minima also reflected in the increase in Dry Conditions indicators. At the same time, a rising rainfall seasonality is inferred from the concurrent increase in Aquatic Taxa and Cyperaceae (Figure 5), even though both summer and winter temperatures became less extreme [55].

Moreover, the sharp increment of Poaceae further supports this trend. This arid transitional phase has been documented by several authors across the western Mediterranean [54,63]. Temperatures also appear to have been cooler during this period [51,52], which may have favoured the expansion of grasslands. Cedar forests would have moved

upwards following the dynamics undertaken in the previous subzone, while *Quercus* pollen kept close to its previous percentages (Figure 5). This may reflect a further stage in the formation of distinct vegetation belts, with *Cedrus* occupying the highest elevations. Below, deciduous oak woodlands may have developed, and at lower altitudes, holm oak (*Quercus ilex*) forests, forming a vertically structured mosaic increasingly resembling the current physiognomy of these mountain ecosystems.

Moreover, this phase reveals a much more abrupt transformation, likely driven by intense human impact. This pronounced shift is not as clearly recorded in other Rif Mountain sequences [15,22,26], suggesting that human influence may have amplified the adverse climatic conditions that led to widespread forest clearance, as indicated by the increase in API [48]. This intensification of human impact may be linked to early activity in high-altitude cedar forests during the Phoenician occupation [34,63] which ultimately brought cedar populations to their lowest recorded levels. The increasingly continuous signal of coprophilous fungi (CFs) and the marked rise in nitrophilous communities (Figure 5) lend further support to this interpretation. Cerealia and *Cannabis* pollen also appear for the first time around ~2800 cal yr BP.

Other effects of the landscape opening at the onset of this subzone include the progressive replacement of *Ilex* by *Cistus* within the Thermophilous Shrubland group, as well as an increased presence of *Pteridium* (Figure 5).

As a result, tree cover, as indicated by the AP/NAP ratio, did not recover but continued to decline, largely due to increasing human activity. The expansion of the Roman Empire appears to have caused a renewed reduction in forests in favour of grasslands, despite climatic conditions that were relatively favourable for forest growth, particularly in terms of temperature. High levels of *Poaceae*, *Perennial pastures* and *Nitrophilous communities* are observed, as well as noticeable levels of shrublands, mainly composed of *Cytisus* and *Erica*, and *Pteridium* (Figure 5). The continuous presence of *Olea* is also noteworthy during this period, although it remains unclear whether it represents wild or cultivated forms under Roman influence [64]. However, both CFs and CHAR remain at low levels, the latter probably linked to the limited extent of tree cover (Figure 5). Interestingly, *Cedrus* shows low but gradually increasing values toward the end of the subzone, suggesting some degree of recovery or stability, likely favoured by more suitable climatic conditions at higher elevations. These conditions may have also contributed to the retreat of evergreen oaks in favour of deciduous ones, possibly reflecting a decrease in climatic seasonality [55]. In fact, human impact was quite mild during this period in the Rif mountains, as Berbers maintained control over forest resources [29,63].

The onset of the Medieval Climate Anomaly (~1400 cal yr BP; [63]) brought warmer and drier conditions to the region [54], a pattern also reflected in our site-specific temperature-precipitation reconstruction around that time (Figure 6). PAR shows a marked increase, suggesting favourable conditions for pollen production, likely associated with thermophilous herbaceous and shrubby taxa. However, tree cover continued to decline, including a moderate retreat of oak forests, particularly deciduous forms. This progressive opening of the landscape appears to have favoured the expansion of *Pteridium* and shrubby communities dominated by *Cistus* (Figure 5). Moreover, *Cedrus* pollen reaches ~9%, suggesting the presence of nearby fragmented stands. This exceeds the ~7% threshold proposed by [49] for local presence in montane settings, although some regional input cannot be entirely ruled out.

Grasslands and nitrophilous communities also expanded, especially from ~1000 cal yr BP onwards, when human impact appears to intensify (Figure 5; [48]), as indicated by the concurrent rise in CHAR, CFs and cultivated taxa such as *Cannabis* and *Vicia* (Figure 5). These human signals may be associated with a period of political instability linked to

Byzantine dominance, the transition to the Idrisid dynasty and the Almoravid conquest of the Rif [29,34,63].

The PCA biplot (Figure 7) illustrates the pronounced vegetation shift characterizing this subzone, with sample scores moving rightward along PC1, reflecting increasing aridity, and upward along PC2, indicating progressive landscape opening. This trajectory is strongly associated with the expansion of anthropogenic taxa and disturbance indicators—such as nitrophilous communities, *Pteridium*, and coprophilous fungi—highlighting the growing impact of human activities.

4.4. Final Collapse of Cedar Forests at Mid-Elevation Under Combined Climatic and Anthropogenic Pressure—Subzone LKHB2 (32–0 cm; ~800 cal yr BP- present)

PAR becomes again low at the beginning of this subzone (Figure 5), indicating unfavourable climatic conditions for pollen production, likely related to the transition from the MCA to the Little Ice Age (LIA), a period marked by dry conditions and cooler temperatures [54,63]. This is further supported by the decline in reconstructed temperature and persistently low precipitation levels observed in our record (Figure 5). The AP/NAP ratio reaches its minimum levels. *Cedrus* also falls to minimum values, while both evergreen and deciduous *Quercus* exhibit a marked decline. The parallel increase in Thermophilous shrubland, Poaceae and *Pteridium* reveals a prominent landscape opening, coupled with a likewise marked increase in nitrophilous communities, CFS and crops like Cerealia, *Cannabis* and *Vicia* (Figure 5). This deforestation episode, observed in other Rifan records [22,25,29,63], may coincide with the rise of the Almohad dynasty (AD ~1150–1250/~800–700 cal. yr BP), a period of intensified forest exploitation, specifically cedar wood [65].

The onset of LIA ~550 cal yr BP [63] would have favoured a slight recovery of tree cover, particularly of cedar forests, as shown by little peaks ~300 cal yr BP. However, successive loggings and other human activities ultimately led to the local collapse of *Cedrus atlantica* at the elevation of LKH, despite the species' well-documented resilience to disturbance [9,15,22]. Cedar forests would only remain in the summits of Jbel Bou Hachem with extremely fragmented populations, as a consequence of the adverse climate conditions and the intensity of human activities. Despite this, cedar woodlands have continued to dominate the vegetation landscape in the easternmost part of the Rif Mountains to the present day [25], demonstrating a strong ecological resilience under current climatic conditions. As shown in the Targuist mire record, *Cedrus atlantica* was able to recover following previous declines when human pressure lessened.

The PCA biplot (Figure 7) places this subzone in the upper right quadrant, with samples showing high scores along both PC1 and PC2, reflecting increasing aridity and progressive landscape opening at mid-elevation. This distribution supports a dual forcing scenario, in which both climatic stress and intensified human activity acted as major drivers of vegetation change, culminating in the degraded open landscape observed today.

The gradual recovery of deciduous oak forests, along with new introductions of *Olea* and *Pinus*, does not prevent AP/NAP from reaching minimum values, due to the continued expansion of grasslands and nitrophilous communities and the peak in CHAR (Figure 5), likely associated with intensive livestock grazing. Evergreen oak forests show a steady decline, as human impact becomes increasingly concentrated at lower elevations. Alongside the intensification of crops such as *Cannabis*, an extensive process of matorralization develops throughout this subzone, driven by increased grazing pressure and fire recurrence [24,66]. The current landscape reveals a slight recovery of tree cover, particularly oak woodlands, although Thermophilous Shrubland and grasslands still dominate [31].

In short, the increase in climatic stress and human impact during the late Meghalayan were likely the main drivers behind the functional collapse of *Cedrus* ecosystems at mid-

elevations in the western Rif Mountains, giving way to more open landscapes dominated by plant formations adapted to drought and rising temperatures. The Merj Lkhil sequence documents this transition in detail. At present, *Cedrus atlantica* is absent from all Moroccan montane sites located below approximately 1300 m a.s.l., and several populations—particularly in the western Rif—have become locally extinct [22,23].

Furthermore, these isolated populations in the western Rif face multiple threats, including their limited spatial extent, intense anthropogenic pressure, and growing exposure to warming trends [28]. Given their genetic distinctiveness, geographic isolation, and the rugged topography of the western Rif, the conservation of these cedar populations is a priority. This complex terrain may provide modern climatic refugia that enhance the species' persistence, making these stands critical for maintaining both regional biodiversity and the long-term viability of *Cedrus atlantica* [28].

The results presented here from Merj Lkhil highlight the vulnerability of cedar populations located at the rear edge of their distribution, in climatically marginal regions, as well as the importance of integrating paleoecological records into conservation strategies. Such studies capture long-term vegetation dynamics and can identify ecological thresholds, providing essential insights into the interactions between society and the environment as key drivers of change.

5. Conclusions

Cedrus reached its maximum extent in the Rif around 7000 cal yr BP, helped by the climate conditions described for the first stages of NOR in the area. A pronounced decline has been observed since 6600 cal yr BP, together with the expansion of oak forests, as a result of increasing aridity. The transition to the MEG exacerbated progressive aridification, which allowed deciduous oak forests to develop at the expense of cedar populations, which would have moved upwards in search of more favourable conditions, given the limited impact of human activity at that time and the ongoing dominant role of climate in shaping vegetation dynamics.

The last three millennia have also been marked by increasing aridity and human influence. The current state of these mountain ecosystems was developing, with the formation of distinct vegetation belts, *Cedrus* occupying the highest altitudes, and human influence potentially intensifying the adverse climatic conditions that resulted in widespread forest clearance.

The increase in climatic stress and human impact during the late Meghalayan were likely the main drivers behind the functional collapse of *Cedrus* ecosystems at mid-elevations in the western Rif Mountains. The conservation of these last cedar populations is a priority if we do not want this iconic mountain conifer to disappear from the Mediterranean landscape.

Supplementary Materials: The following supporting information can be downloaded at: https://www.mdpi.com/article/doi/s1, Figure S1: Detailed pollen diagram of LKH.

Author Contributions: F.A.-S. received funding to carry out the research. F.A.-S. and J.A.L.-S. designed the research; F.A.-S., J.A.L.-S., D.A.-S., S.P.-D. and A.G.-H. collected the core and analyzed the paleoecological data; D.R.-R. performed palaeoclimatical reconstructions and analyzed the data; F.A.-S. and D.A.-S. led the writing of the manuscript. All authors have read and agreed to the published version of the manuscript.

Funding: This publication is part of the project I + D + i TED2021-132631B-I00 funded by MICIU/AEI/10.13039/501100011033 and by NextGenerationEU/PRTR.

Data Availability Statement: The data presented in this study are openly available DIGIBUG at https://digibug.ugr.es/ (accessed on 6 August 2025).

Conflicts of Interest: The authors declare no conflicts of interest.

References

1. Myers, N.; Mittermeier, R.A.; Mittermeier, C.G.; da Fonseca, G.A.B.; Kent, J. Biodiversity hotspots for conservation priorities. *Nature* **2000**, *403*, 853–858. https://doi.org/10.1038/35002501.
2. Körner, C. The use of 'altitude' in ecological research. *Trends Ecol. Evol.* **2007**, *22*, 569–574. https://doi.org/10.1016/j.tree.2007.09.006.
3. Tito, R.; Vasconcelos, H.L.; Feeley, K.J. Mountain Ecosystems as Natural Laboratories for Climate Change Experiments. *Front. For. Glob. Change* **2020**, *3*, 38. https://doi.org/10.3389/ffgc.2020.00038.
4. IUCN. *Mediterranean Mountains in a Changing World. Guidelines for Developing Action Plans*; Regato, P., Salman, R., Eds.; IUCN: Gland, Switzerland; Malaga, Spain, 2008.
5. Médail, F.; Quézel, P. Biodiversity hotspots in the Mediterranean Basin: Setting global conservation priorities. *Conserv. Biol.* **1999**, *13*, 1510–1513.
6. Elenga, H.; Peyron, O.; Bonnefille, R.; Prentice, I.C.; Jolly, D.; Cheddadi, R.; Guiot, J.; Andrieu, V.; Bottema, S.; Buchet, G.; et al. Pollen-based reconstruction for southern Europe and Africa 18 000 years ago. *J. Biogeogr.* **2000**, *27*, 621–634. https://doi.org/10.1046/j.1365-2699.2000.00430.x.
7. Kunert, N.; Hajek, P.; Hietz, P.; Morris, H.; Rosner, S.; Tholen, D. Summer temperatures reach the thermal tolerance threshold of photosynthetic decline in temperate conifers. *Plant Biol.* **2022**, *24*, 1254–1261.
8. Linares, J.C.; Tíscar, P.A.; Camarero, J.J.; Taiqui, L.; Viñegla, B.; Seco, J.; José, M.; Carreira, J.A. Tree growth decline on relict Western-Mediterranean mountain forests: Causes and impacts. In *Forest Decline: Causes and Impacts*; Jenkins, J.J., Ed.; Nova Science Publishers, Inc.: Hauppauge, NY, USA, 2011.
9. Camarero, J.J.; Sánchez-Salguero, R.; Sangüesa-Barreda, G.; Lechuga, V.; Viñegla, B.; Seco, J.I.; Taiqui, L.; Carreira, J.A.; Linares, J.C. Drought, axe and goats. More variable and synchronized growth forecasts worsening dieback in Moroccan Atlas cedar forests. *Sci. Total Environ.* **2021**, *765*, 142752. https://doi.org/10.1016/j.scitotenv.2020.142752.
10. Woodward, J.C. *The Physical Geography of the Mediterranean*; Oxford University Press: Oxford, UK, 2009.
11. Kuennecke, B.H. *Temperate Forest Biomes*; Bloomsbury Publishing: New York, NY, USA, 2008.
12. Loidi, J.; Navarro-Sánchez, G.; Vynokurov, D. Climatic definitions of the world's terrestrial biomes. *Veg. Classif. Surv.* **2022**, *3*, 231–271.
13. Faber-Langendoen, D.; Keeler, T.; Meidinger, D.; Josse, C.; Weakley, A.; Tart, D.; Navarro, G.; Hoagland, B.; Ponomarenko, S.; Fults, G.; Helmer, E. *Classification and Description of World Formation Types*; U.S. Department of Agriculture, Forest Service, Rocky Mountain Research Station: Fort Collins, CO, USA, 2016.
14. Benabid, A. Les écosystèmes forestiers, préforestiers et presteppiques du Maroc: Diversité, repartition biogéographique et problèmes posés par leur aménagement. *Forêt Méditerranéenne* **1985**, *VII*, 53-64.
15. Cheddadi, R.; Henrot, A.J.; François, L.; Boyer, F.; Bush, M.; Carre, M.; Coissac, E.; De Oliveira, P.E.; Ficetola, F.; Hambuckers, A.; et al. Microrefugia, climate change, and conservation of Cedrus atlantica in the Rif Mountains, Morocco. *Front. Ecol. Evol.* **2017**, *5*, 114. https://doi.org/10.3389/fevo.2017.00114.
16. Cheddadi, R.; Nourelbait, M.; François, L.; Fady, B.; Lefèvre, F.; Khater, C. Come rain or come shine, the species richness will decline in the Moroccan mountains. *Glob. Ecol. Conserv.* **2024**, *52*, e02986. https://doi.org/10.1016/j.gecco.2024.e02986.
17. Mazzoleni, S.; Di Pasquale, G.; Mulligan, M.; Di Martino, P.; Rego, F. (Eds.) *Recent Dynamics of the Mediterranean Vegetation and Landscape*; John Wiley & Sons: Chichester, UK, 2004.
18. Thomas, P. Cedrus atlantica. In IU*CN Red List of Threatened Species, Version 2013.1*; IUCN: Gland, Switzerland, 2013 https://doi.org/10.2305/IUCN.UK.2013-1.RLTS.T42303A2970716.en.
19. Linstädter, J.; Kehl, M.; Broich, M.; López-Sáez, J.A. Chronostratigraphy, site formation processes and pollen record of Ifri n'Et-sedda, NE Morocco. *Quatern. Int.* **2016**, *410*, 6–29. https://doi.org/10.1016/j.quaint.2015.11.017.
20. Ruiz-Alonso, M.; Abel-Schaad, D.; López-Sáez, J.A.; Martínez Sánchez, R.M.; Vera-Rodríguez, J.C.; Pérez-Jordàn, G.; Peña-Chocarro, L.; Alba-Sánchez, F. Late glacial–postglacial North African landscape and forest management: Palynological and anthracological studies in the caves of Kaf Taht el-Ghar and El Khil (Tingitana Peninsula, Morocco). *Rev. Palaeobot. Palyno.* **2021**, *293*, 104486.

21. Zapata, L.; López-Sáez, J.A.; Ruiz-Alonso, M.; Linstädter, J.; Pérez-Jordà, G.; Morales, J.; Kehl, M.; Peña-Chocarro, L. Holocene environmental change and human impact in NE Morocco: Palaeobotanical evidence from Ifri Oudadane. *Holocene* **2013**, *23*, 1286–1296. https://doi.org/10.1177/0959683613486944.
22. Abel-Schaad, D.; Iriarte, E.; López-Sáez, J.A.; Pérez-Díaz, S.; Ruiz, S.S.; Cheddadi, R.; Alba-Sánchez, F. Are Cedrus atlantica forests in the Rif Mountains of Morocco heading towards local extinction? *Holocene* **2018**, *28*, 1023–1037.
23. Cheddadi, R.; Bouaissa, O.; Rhoujjati, A.; Dezileau, L. Environmental changes in the Moroccan western Rif mountains over the last 9,000 years. *Quaternaire* **2016**, *27*, 15–25. https://doi.org/10.4000/quaternaire.7517.
24. Barbero, M.; Bonin, G.; Loisel, R.; Quézel, P. Changes and disturbances of forest ecosystems caused by human activities in the western part of the Mediterranean basin. *Vegetatio* **1990**, *87*, 151–173. https://doi.org/10.1007/BF00042952.
25. Abel-Schaad, D.; Sabariego-Ruiz, S.; Lopez Saez, J.A.; Alba-Sanchez, F. 69. Targuist mire (Central Rif, Morocco). *Grana* **2023**, *62*, 218–220. https://doi.org/10.1080/00173134.2023.2222118.
26. Abel-Schaad, D.; Alba-Sanchez, F.; Lopez Saez, J.A.; Gonzalez-Hernandez, A.; Martin-Girela, M.I.; Cheddadi, R. 78. Fouara (Western Rif, Morocco). *Grana* **2024**, *63*, 402–404. https://doi.org/10.1080/00173134.2024.2429989.
27. Birks, H.J.B. Contributions of Quaternary botany to modern ecology and biogeography. *Plant Ecol. Divers.* **2019**, *12*, *3–4*, 189-385. https://doi.org/10.1080/17550874.2019.1646831.
28. Cheddadi, R.; Taberlet, P.; Boyer, F.; Coissac, E.; Rhoujjati, A.; Urbach, D.; Remy, C.; Khater, C.; el Antry, S.; Aoujdad, J.; et al. Priority conservation areas for Cedrus atlantica in the Atlas Mountains, Morocco. *Conserv. Sci. Pract.* **2022**, *4*, e12680. https://doi.org/10.1111/csp2.12680.
29. Muller, S.D.; Rhazi, L.; Andrieux, B.; Bottollier-Curtet, M.; Fauquette, S.; Saber, E.-R.; Rifai, N.; Daoud-Bouattour, A. Vegetation history of the western Rif Mountains (NW Morocco): Origin, late-Holocene dynamics and human impact. *Veg. Hist. Archaeobot.* **2015**, *24*, 487–501. https://doi.org/10.1007/s00334-014-0504-9.
30. Muller, S.D.; Daoud-Bouattour, A.; Fauquette, S.; Bottollier-Curtet, M.; Rifai, N.; Robles, M.; Saber, E.-R.; El Madihi, M.; Moukrim, S.; Rhazi, L. Holocene history of peatland communities of central Rif (Northern Morocco). *Geobios* **2022**, *70*, 35–53. https://doi.org/10.1016/j.geobios.2021.12.001.
31. Ajbilou, R.; Marañón, T.; Arroyo, J. Ecological and biogeographical analyses of Mediterranean forests of northern Morocco. *Acta Oecol.* **2006**, *29*, 104–113. https://doi.org/10.1016/j.actao.2005.08.006.
32. Benabid, A. Bref aperçu sur la zonation altitudinale de la végétation climacique du Maroc. *Ecol. Mediterr.* **1982**, *8*, 301–315. https://doi.org/10.3406/ecmed.1982.1956.
33. Charco, J. *El Bosque Mediterráneo en el Norte de África: Biodiversidad y Lucha Contra la Desertización*; Agencia Española de Cooperación: Madrid, Spain, 1999.
34. Taiqui, L.; Cantarino, C.M. Eléments historiques d'analyse écologique des paysages montagneux du Rif Occidental (Maroc). Mediterranea. *Ser. De Estud. Biológicos* **1997**, *16*, 23–35.
35. Carrión Marco, Y.; Vidal-Matutano, P.; Morales, J.; Henríquez Valido, P.; Potì, A.; Kehl, M.; Linstädter, J.; Weniger, G.-C.; Mikdad, A. Late glacial landscape dynamics based on macrobotanical data: Evidence from Ifri El Baroud (NE Morocco). *Environ. Archaeol*. **2021**, *26*, 131–145. https://doi.org/10.1080/14614103.2018.1538088.
36. Barton, R.N.E.; Collcutt, S.N.; Carrión Marco, Y.; Clark-Balzan, L.; Debenham, N.D.; Morales-Mateos, J.; Bouzouggar, A. Reconsidering the MSA to LSA transition at Taforalt Cave (Morocco) in the light of new multi-proxy dating evidence. *Quat. Int.* **2016**, *413*, 36–49. https://doi.org/10.1016/j.quaint.2015.11.085.
37. Reimer, P.J.; Austin, W.E.N.; Bard, E.; Babyliss, A.; Blackwell, P.G.; Ramsey, C.B.; Butzin, M.; Cheng, H.; Edwards, R.L.; Friedrich, M.; et al. The IntCal20 Northern Hemisphere Radiocarbon Age Calibration Curve (0–55 cal kBP). *Radiocarbon* **2020**, *62*, 725–757. https://doi.org/10.1017/RDC.2020.41.
38. Blaauw, M. Methods and code for 'classical' age-modelling of radiocarbon sequences. *Quat. Geochronol.* **2010**, *5*, 512–518. https://doi.org/10.1016/j.quageo.2010.01.002.
39. Faegri, K.; Iversen, J. *Textbook of Pollen Analysis*; John Wiley and Sons: Chichester, UK, 1989.
40. Goeury, C.; de Beaulieu, J.L. A propos de la concentration du pollen à l'aide de la liqueur de Thoulet dans les sédiments minéraux. *Pollen Et Spores* **1979**, *21*, 239–251.
41. Stockmarr, J. Tablets with spores used in absolute pollen analysis. *Pollen Et Spores* **1971**, *13*, 614–621.
42. Moore, P.D.; Webb, J.A.; Collinson, M.E. *Pollen Analysis*; Blackwell: Oxford, UK, 1991.
43. Reille, M. *Pollen et Spores d'Europe et d'Afrique du Nord*, 2nd ed.; Laboratoire de Botanique Historique et Palynologie: Marseille, France, 1999.

44. Miola, A. Tools for Non-Pollen Palynomorphs (NPPs) analysis: A list of Quaternary NPP types and reference literature in English language (1972–2011). *Rev. Palaeobot. Palynol.* **2012**, *186*, 142–161. https://doi.org/10.1016/j.revpalbo.2012.06.010.
45. Mooney, S.D.; Tinner, W. The analysis of charcoal in peat and organic sediments. *Mires Peat* **2011**, *7*, 1–18.
46. Long, C.J.; Whitlock, C. Fire and vegetation history from the coastal rain forest of the western Oregon Coast Range. *Quat. Res.* **2002**, *58*, 215–225. https://doi.org/10.1006/qres.2002.2378.
47. Hammer, Ø.; Harper, D.A.T.; Ryan, P.D. PAST: Paleontological statistics software package for education and data analysis. *Palaeontol. Electron.* **2001**, *4*, 9. Available online: http://palaeo-electronica.org/2001_1/past/issue1_01.htm (accessed on 29 September 2023).
48. Cheddadi, R.; Palmisano, A.; López-Sáez, J.A.; Nourelbait, M.; Zielhofer, C.; Tabel, J.; Rhoujjati, A.; Khater, C.; Woodbridge, J.; Lucarini, G.; et al. Human demography changes in Morocco and environmental imprint during the Holocene. *Holocene* **2019**, *29*, 816–829. https://doi.org/10.1177/0959683619826657.
49. Bell, B.A.; Fletcher, W.J. Modern surface pollen assemblages from the Middle and High Atlas, Morocco: Insights into pollen representation and transport. *Grana* **2016**, *55*, 286–301. https://doi.org/10.1080/00173134.2015.1108996.
50. Romera-Romera, D.; Alba-Sánchez, F.; Abel-Schaad, D.; Nieto-Lugilde, D. Replicable fine-spatio-temporal climate data for long-term ecology in the Western Mediterranean. *Sci. Data* **2025**, *12*, 747. https://doi.org/10.1038/s41597-025-05067-9.
51. Cacho, I.; Grimalt, J.O.; Canals, M.; Sbaffi, L.; Shackleton, N.J.; Schönfeld, J.; Zahn, R. Variability of the western Mediterranean Sea surface temperature during the last 25,000 years and its connection with the Northern Hemisphere climatic changes. *Paleoceanography* **2001**, *16*, 40–52. https://doi.org/10.1029/2000PA000502.
52. Kim, J.H.; Meggers, H.; Rimbu, N.; Lohmann, G.; Freudenthal, T.; Mu, P.J.; Schneider, R.R. Impacts of the North Atlantic gyre circulation on Holocene climate off northwest Africa. *Geology* **2007**, *35*, 387–390. https://doi.org/10.1130/G23251A.1.
53. Zielhofer, C.; Fletcher, W.J.; Mischke, S.; de Batist, M.; Campbell, J.F.E.; Joannin, S.; Tjallingii, R.; El Hamouti, N.; Junginger, A.; Stele, A. et al. Atlantic forcing of Western Mediterranean winter rain minima during the last 12,000 years. *Quat. Sci. Rev.* **2017**, *157*, 29–51. https://doi.org/10.1016/j.quascirev.2016.11.037.
54. Nieto-Moreno, V.; Martínez-Ruiz, F.; Giralt, S.; Jiménez-Espejo, F.; Gallego-Torres, D.; Rodrigo-Gámiz, M.; García-Orellana, J.; Ortega-Huertas, M.; de Lange, G.J. Tracking climate variability in the western Mediterranean during the Late-Holocene: A multiproxy approach. *Clim. Past* **2011**, *7*, 1395–1414. https://doi.org/10.5194/cp-7-1395-2011.
55. Laskar, J.; Robutel, P.; Joutel, F.; Gaustineau, M.; Correia, A.C.M.; Levrard, B. A long-term numerical solution for the insolation quantities of the Earth. *Astron. Astrophys.* **2004**, *428*, 261–285. https://doi.org/10.1051/0004-6361:20041335.
56. Walker, M.; Head, M.J.; Lowe, J.; Berkelhammer, M.; Björck, S.; Cheng, H.; Cwynar, L.C.; Fisher, D.; Gkinis, V.; Long, A.; et al. Subdividing the Holocene Series/Epoch: Formalization of stages/ages and subseries/subepochs, and designation of GSSPs and auxiliary stratotypes. *J. Quat. Sci.* **2019**, *34*, 173–186. https://doi.org/10.1002/jqs.3097.
57. Trouet, V.; Esper, J.; Graham, N.E.; Baker, A.; Scourse, J.D.; Frank, D.C. Persistent positive North Atlantic Oscillation mode dominated the Medieval Climate Anomaly. *Science* **2009**, *324*, 78–80. https://doi.org/10.1126/science.1166349.
58. Linstädter, J.; Broich, M.; Weninger, B. Defining the Early Neolithic of the Eastern Rif, Morocco–Spatial distribution, chronological framework and impact of environmental changes. *Quatern. Int.* **2018**, *472*, 272–282. https://doi.org/10.1016/j.quaint.2016.07.042.
59. Leroy, S.A.; Freitas, M.C.; Andrade, C.; Cearreta, A.; Maanan, M.; Costa, P. A~ 6,600 year history of vegetation changes and sediment infill of the Moulay Bousselham Lagoon, Atlantic Morocco. *J. Afr. Earth Sci.* **2025**, *223*, 105492. https://doi.org/10.1016/j.jafrearsci.2024.105492.
60. Gottfried, M.; Pauli, H.; Futschik, A.; Akhalkatsi, M.; Barančok, P.; Alonso, J.L.B.; Coldea, G.; Dick, J.; Erschbamer, B.; Calzado, R.F.; et al. Continent-wide response of mountain vegetation to climate change. *Nat. Clim. Change* **2012**, *2*, 111–115. https://doi.org/10.1038/nclimate1329.
61. Campbell, J.F.; Fletcher, W.J.; Joannin, S.; Hughes, P.; Rhanem, M.; Zielhofer, C. Environmental drivers of Holocene forest development in the Middle Atlas, Morocco. *Front. Ecol. Evol.* **2017**, *5*, 113. https://doi.org/10.3389/fevo.2017.00113.
62. Leunda, M.; González-Sampériz, P.; Gil-Romera, G.; Aranbarri, J.; Moreno, A.; Oliva-Urcia, B.; Sevilla-Callejo, M.; Valero-Garcésa, B. The Late-Glacial and Holocene Marboré Lake sequence (2612 m asl, Central Pyrenees, Spain): Testing high altitude sites sensitivity to millennial scale vegetation and climate variability. *Glob. Planet Change* **2017**, *157*, 214–231. https://doi.org/10.1016/j.gloplacha.2017.08.008.
63. Martín-Puertas, C.; Jiménez-Espejo, F.; Martínez-Ruiz, F.; Nieto-Moreno, V.; Rodrigo, M.; Mata, M.P.; Valero-Garcés, B.L. Late-Holocene climate variability in the southwestern Mediterranean region: An integrated marine and terrestrial geochemical approach. *Clim. Past* **2010**, *6*, 807–816. https://doi.org/10.5194/cp-6-807-2010.

64. Langgut, D.; Cheddadi, R.; Carrión, J.S.; Cavanagh, M.; Colombaroli, D.; Eastwood, W.J.; Greenberg, R.; Litt, T.; Mercuri, A.M.; Miebach, A.; et al. The origin and spread of olive cultivation in the Mediterranean Basin: The fossil pollen evidence. *Holocene* **2019**, *29*, 902–922. https://doi.org/10.1177/0959683619826654.
65. Park, T.K.; Boum, A. *Historical Dictionary of Morocco*; Scarecrow Press: Lanham, MD, USA, 2005.
66. Cheddadi, R.; Nourelbait, M.; Bouaissa, O.; Tabel, J.; Rhoujjati, A.; López-Sáez, J.A.; Alba-Sánchez, F.; Khater, C.; Ballouche, A.; Dezileau, L.; et al. A history of human impact on Moroccan mountain landscapes. *Afr. Archaeol. Rev.* **2015**, *32*, 233–248. https://doi.org/10.1007/s10437-015-9186-7.